

START-TO-END SIMULATIONS FOR HEAVY-ION ACCELERATOR OF RISF

Eun-San Kim*, JungBae Bahng, Ji-Gwang Hwang, Si-Won Jang,
Kyungpook National Univ., Deagu, Korea,

Bong-Hyuk Choi, Hye-Jin Kim, Hyung-Jin Kim, Dong-O Jeon, IBS, Daejeon, Korea

Abstract

RAON has been designed as a facility for a rare isotope accelerator at RISF. The accelerator for in-flight system accelerates uranium and proton beams to 200 MeV/u and 600 MeV, respectively, with beam power of 400 kW. Front-end system consists of two 28 GHz ECR-IS with 10 keV/u, LEBT with two 90 degree bends and multi-harmonic buncher with three different rf frequencies, RFQ with 81.25 MHz and 500 keV/u, and MEFT with two re-bunchers. The driver linac system design has been performed to optimize the beam and accelerator parameters to meet the required design goals. HEBT delivers the ion beams from Linac to in-flight target. For these designs, we have performed start-to-end simulations with the beams from LEBT to HEBT by using 1 M macroparticles. We present the design performance and results of the beam dynamics. Our simulation results shows that transmission rates of Uranium and proton beams are 81 % and 87 %, respectively, from LEBT to HEBT. The condition of beam losses below 1 W/m is achieved by the designed facility.

INTRODUCTION

RISF (Rare Isotope Science Project) is designed to accelerate the ions from proton to uranium for 400 kW in-flight system. The accelerator also includes a post-accelerator to provide user facilities with rare isotope beams by ISOL system. Fig. 1 shows layout for the entire accelerator systems.

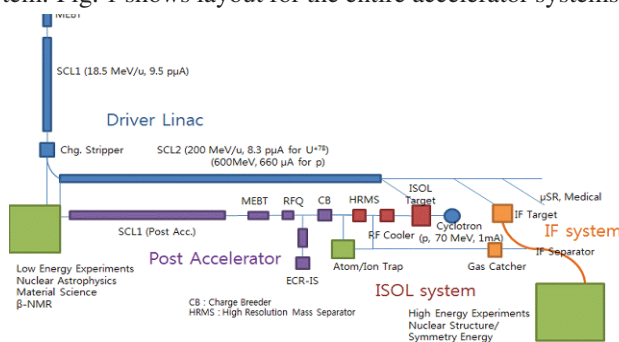


Figure 1: Layout for RAON accelerator.

LEBT

The LEBT with achromatic optics consists of two 90-degree bends, pair-solenoids for beam matching with ECR-IS and RFQ, multi-harmonic buncher, velocity equalizer, steering magnets, collimation systems, chopper and diagnostics. Fig.2 shows the layout of the LEBT for driver

*eskim1@knu.ac.kr

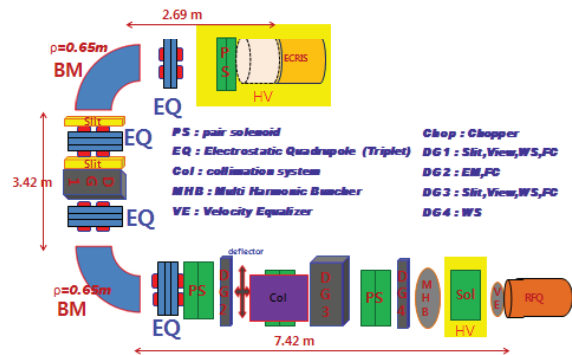


Figure 2: Layout of the front-end system for the drive linac.

linac. Fig. 3 shows the designed optics and beam envelopes for the LEBT by TRANSPORT code. The dc beam from the ECR-IS is bunched before injection into the RFQ. Multi-harmonic buncher (MHB) with three different rf frequencies is applied to get a short bunch length with high bunching efficiency. To perform the beam simulations, IMPACT-Z code is utilized for 6-dimension tracking that includes the effect of space-charge force[1]. A normalized rms emittance of 0.08π mm-mrad and intrinsic energy spread of 0.05% are considered as initial beams. 1 M macro-particles are initially generated in 4-dimensional water-bag transverse distributions with uniform longitudinal distributions in phase spaces and are tracked in the simulations[2].

Fig. 4 shows the (top) initial horizontal, vertical and longitudinal beam distributions for two-charge state beam of $^{238}\text{U}^{33+}$ (blue) and $^{238}\text{U}^{34+}$ (red) with $400 e\mu\text{A}$ and 10 keV/u. Fig. 4 also shows the beam distributions (middle) at the entrance of RFQ and the beam envelop (bottom) in the designed LEBT. Two-charge state beam due to the MHB with the fundamental frequency of 40.625 MHz is bunched as well as longitudinally separated from each other due to velocity difference. Velocity equalizer (VE) is used to provide each of two-charge state beams with the same velocity at the entrance of RFQ. A distance between MHB and VE is given by 1.18 m, which corresponds to the two-charge state beam of $^{238}\text{U}^{33+}$ and $^{238}\text{U}^{34+}$.

The cores of the two-charge state beams well overlap and tail particles increases the beam emittance. The simulation shows that the designed LEBT under the effect of space-charge force provides good beam matching and bunching for the two-charge state beam. It is shown that the space-charge effect for the uranium beam of the $400 e\mu\text{A}$ is small in the LEBT. The LEBT shows the beam transmission of 99.8 % and emittance growth of 9.8 %.

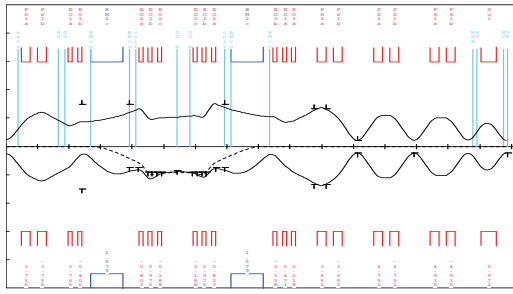


Figure 3: Designed optics and envelopes for LEBT.

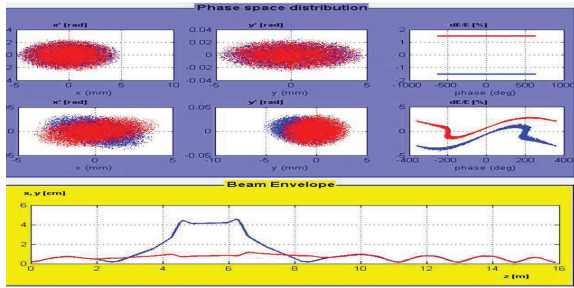


Figure 4: (top) Initial beam distributions, (middle) beam distributions at the entrance of RFQ and (bottom) beam envelopes in the LEBT.

RFQ

The RFQ is designed to accelerate the beam with two-charge states ($^{238}\text{U}^{33+}$ and $^{238}\text{U}^{34+}$) beams from 10 keV/u to 500 keV/u. PARMTEQ is used to get the RFQ design parameters. Charge state of 33.5 in PARMTEQ is used for two-charge state beam of the Uranium.

The vane voltage is designed to change from 70 kV to 124 kV in the RFQ. Number of radial matching cell is 5 and accelerating efficiency is fixed to be 0.58. The synchronous phase becomes to -30 degrees at the end of gentle buncher from -90 degrees at the entrance of the RFQ. The modulation factor increases from 1 to about 2. The total length of RFQ is 5.3 m and number of cell is 247. The maximum peak surface electric field E is 17 MV/m that corresponds to $1.67E_k$, where E_k is the Kilpatrick criterion.

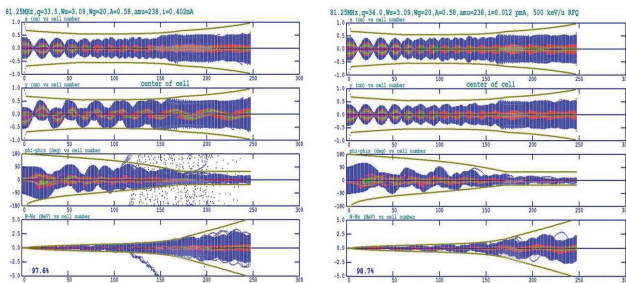


Figure 5: Beam envelopes, phase deviation and kinetic energy deviation along RFQ. Left and right denote the results for 33+ and 34+ charge in Uranium beam, respectively.

Fig. 5 shows the transverse envelopes, phase deviation and kinetic energy deviation as a function of cell number

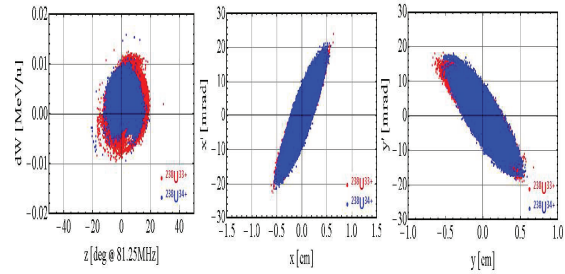


Figure 6: Beam distributions at the exit of RFQ.

for the single charge state of +33 (left) and +34 (right) in Uranium beam. When the beam from the LEBT is tracked by the RFQ, the beam transmission rate is 97.5% and normalized rms transverse emittances of output beam are $\epsilon_x = 0.11 \pi$ mm-mrad and $\epsilon_y = 0.13 \pi$ mm-mrad, and longitudinal emittance is 1.8 MeV-deg. Fig. 6 shows the beam distributions in phase space at the exit of RFQ.

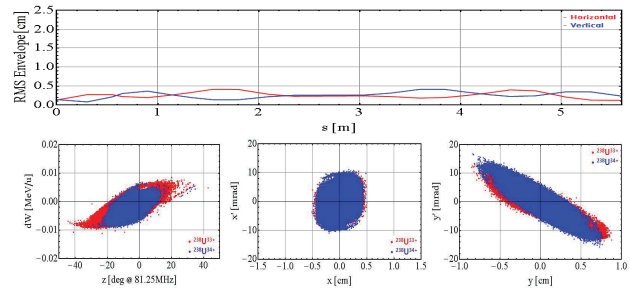


Figure 7: (top) Beam envelopes and (bottom) beam distributions at the exit of MEBT.

MEBT

The Medium Energy Beam Transport (MEBT) system requires to match the optical parameters with linac in transverse plane and also remove the unaccelerated ion beams from the RFQ linac. The optics design of the MEBT system is performed by using TRACE3D code and particle tracking is performed by using TRACK code[3]. Five room temperature quadrupole magnets are used to minimize the transverse emittance growth of two-charge state beams. Two rebunchers are used to provide flexible longitudinal matching from the exit of the RFQ to the entrance of the superconducting linac. The quadrupole magnets have a field of less than 0.5 T at the pole-tip. Rf frequency of rebuncher has 81.25 MHz and $\beta_{opt} = 0.025$. When the beam from the LEBT is tracked to the MEBT, the beam transmission rate is 100% and emittance growth is negligible. Fig.7 shows the (top) beam envelopes in MEBT and (bottom) beam distributions at the exit of MEBT.

SUPERCONDUCTING LINAC

The linac section consists of Linac-1, charge stripper section and Linac-2. Linac-1 consists of QWR and HWR cavities, where 1 cryomodule for QWR includes 1 cavity and 1 cryomodule for HWR includes 3 or 6 cavities.

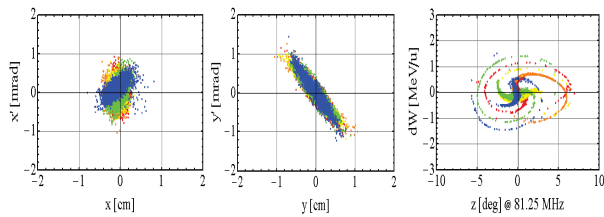


Figure 8: Beam distributions at the exit of LIANC.

Linac-2 consists of SSR1 and SSR2, where 1 cryomodule for SSR1 includes 4 cavities and 1 cryomodule for SSR2 includes 8 cavities[4].

Beam dynamic simulations are performed by Linac-1, charge stripping section and Linac-2 by utilizing the Uranium beam from the LEBT. The charge-stripping section includes charge strippers, 90 degree bending section and matching section with Linac-2. It also includes 3 re-bunchers that lead to acceptable longitudinal emittance growth. Fig. 8 shows the beam distributions in phase spaces at the exit of linac by TRACK code. Beam energy in Linac-1 and final energy of Uranium beam is 18.6 MeV/u and 200 MeV/u, respectively. Beam transmission rate in the whole linac is 83 %. Normalized rms transverse emittances of output beam are $\epsilon_x = 0.195 \pi$ mm-mrad and $\epsilon_y = 0.196 \pi$ mm-mrad, and longitudinal emittance is 39 MeV-degree when solid carbon stripper is included. Fig.9 shows the rms transverse (top) and longitudinal (bottom) emittances in the linac. Fig.10 shows the rms beam envelope (top) and rms bunch length (bottom) in the linac when the beam from LEBT is used.

Start-to-end simulations for proton beam is also performed. Fig.11 shows the beam distributions at the exit of linac when proton beam from the LEBT is used. Initial beam emittances at LEBT are $\epsilon_x = 0.15 \pi$ mm-mrad and $\epsilon_y = 0.15 \pi$ mm-mrad. Final energy of proton beam is 620 MeV and beam transmission rate from LEBT to linac is 87.8 %. Normalized rms transverse emittances of output beam are $\epsilon_x = 0.24 \pi$ mm-mrad and $\epsilon_y = 0.26 \pi$ mm-mrad, and longitudinal emittance is 0.032 MeV-degree.

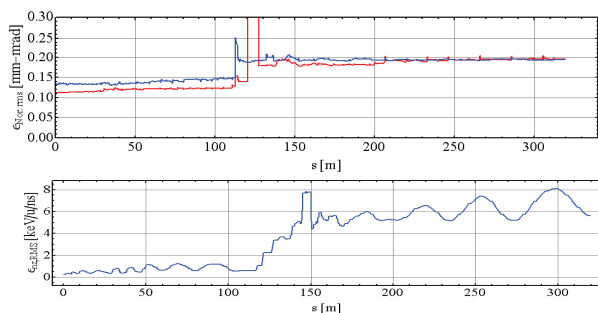


Figure 9: Rms transverse (top) and longitudinal emittances (bottom) in the linac when the beam from LEBT is used.

HEBT

The HEBT (high-energy beam transport) line with 29 m long delivers Uranium beams from Linac-2 to fragmenta-

ISBN 978-3-95450-122-9

1960

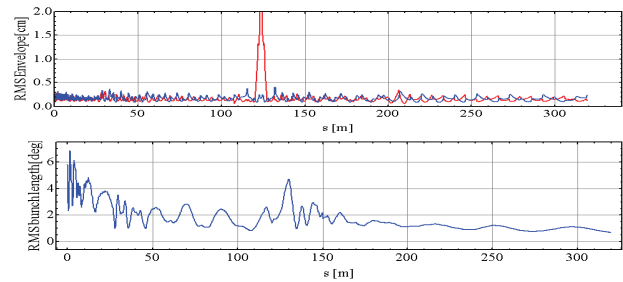


Figure 10: Rms beam envelope and rms bunch length in the linac when the beam from LEBT is used.

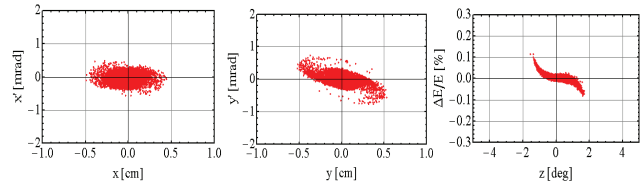


Figure 11: Beam distributions at the exit of linac when the proton beam from LEBT is used.

tion target. The system is designed to achieve efficient delivery of multi-charge states beam with a small beam size of around 1 mm rms and full pulse length of 1 ns on target. Achromatic bending sections with sextupoles are used to compensate high chromatic aberrations in the HEBT. Fig. 12 shows the beam distributions in phase space at the exit of HEBT.

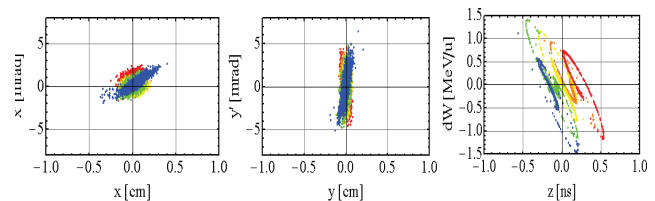


Figure 12: Beam distributions at the exit of the HEBT.

SUMMARY

Start-to-end beam simulations at RAON are performed to optimize from the LEBT to HEBT. It shows that the performance results exist within scope of the requirements by RAON. The simulation results also show satisfactory control of beam losses in the Front-End and linac system. In addition to start-to-end simulations for the driver linac, start-to-end beam simulations for both re-accelerator and Linac-2 have being also performed.

REFERENCES

- [1] J. Qiang et al., J. Comput. Phys. 163 p. 434 (2000).
- [2] Eun-San Kim, et al., TUPWO037, these proceedings.
- [3] P. Ostroumov and K. Shepard, Phys. Rev. ST. Accel. Beams 4, 110101 (2001).
- [4] Hyung-Jin Kim, et al., THPW064, these proceedings.

05 Beam Dynamics and Electromagnetic Fields

D01 Beam Optics - Lattices, Correction Schemes, Transport